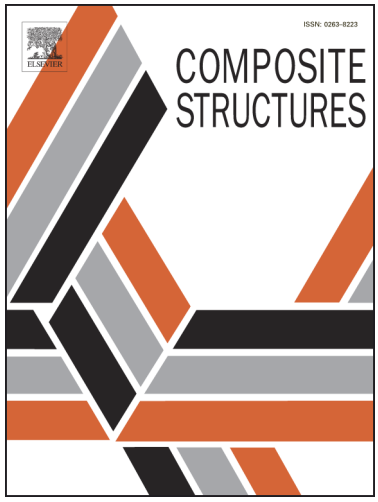

Influence of Infill Concrete Strength on the Flexural Behaviour of Pultruded GFRP Square Beams

Majid Muttashar, Allan Manalo, Warna Karunasena, Weena Lokuge

PII: S0263-8223(16)30112-X
DOI: http://dx.doi.org/10.1016/j.compstruct.2016.02.071
Reference: COST 7284

To appear in: *Composite Structures*

Please cite this article as: Muttashar, M., Manalo, A., Karunasena, W., Lokuge, W., Influence of Infill Concrete Strength on the Flexural Behaviour of Pultruded GFRP Square Beams, *Composite Structures* (2016), doi: http://dx.doi.org/10.1016/j.compstruct.2016.02.071

RESEARCH PAPER

Influence of Infill Concrete Strength on the Flexural Behaviour of Pultruded GFRP Square Beams

(Title contains 14 words)

Running headline: Influence of Infill Concrete Strength on the Flexural Behaviour of Pultruded GFRP Square Beams
(81 characters)

by

Majid Muttashar[1, 2], Allan Manalo[1], Warna Karunasena[1] and Weena Lokuge[1]
[1] Centre of Excellence in Engineered Fibre Composites (CEEFC),
School of Civil Engineering and Surveying, University of Southern Queensland, Toowoomba 4350, Australia
[2] Department of Civil Engineering, College of Engineering, University of Thi Qar, Iraq.

Submitted to
Composite Structures

Corresponding Author:

Weena Lokuge
Lecturer in Civil Engineering
Centre of Excellence in Engineered Fibre Composites (CEEFC),
School of Civil Engineering and Surveying,
University of Southern Queensland,
Toowoomba, Queensland 4350, Australia
Tel: +61 7 3470 4477 Fax: +61 7 4631 2526
E-mail: weena.lokuge@usq.edu.au

Manuscript summary:

Total pages	17 (including cover page)
Number of figures	14
Number of tables	3

Influence of Infill Concrete Strength on the Flexural Behaviour of Pultruded GFRP Square Beams

Majid Muttashar[1, 2], Allan Manalo[1], Warna Karunasena[1] and Weena Lokuge[1, *]

[1] Centre of Excellence in Engineered Fibre Composites (CEEFC), School of Civil Engineering and Surveying, University of Southern Queensland, Toowoomba 4350, Australia

[2] Department of Civil Engineering, College of Engineering, University of Thi Qar, Iraq.

Email: majid.alzaidy@gmail.com, allan.manalo@usq.edu.au, karu.karunasena@usq.edu.au, weena.lokuge@usq.edu.au

Abstract

This paper presents experimental and analytical studies on the effect of the compressive strength of the concrete infill on the flexural behaviour of composite beams. Hollow pultruded Glass Fibre Reinforced Polymer (GFRP) square beams (125 mm x125 mm x 6.5 mm) filled with concrete having 10, 37 and 43.5 MPa compressive strength were tested under static four-point bending. The results indicate that filled GFRP beams failed at a load 100 to 141% higher than hollow beams and showed 25% increase in stiffness. However, the increase in concrete compressive strength from 10 to 43.5 MPa increased the ultimate load by only 19% but exhibited almost the same flexural stiffness indicating that a low strength concrete is a practical solution to fill the GFRP profiles to be used as beam applications. Moreover, the concrete infill prevented the premature buckling and web crushing of the GFRP tube. The maximum strain measured at failure is similar to the compressive strain determined from the coupon test indicating the effective utilisation of the GFRP material. Finally, Fibre Model Analysis which considered the partial confined stress – strain curve for the concrete infill gave an accurate prediction of the flexural behaviour of the concrete filled GFRP sections.

Keywords: Composite beam, flexural confinement, failure load, GFRP, concrete strength, flexural behaviour

*Corresponding author, tel. +61 7 3470 4477; fax. +61 7 4631 2526
E-mail addresses: weena.lokuge@usq.edu.au (Weena Lokuge), majid.alzaidy@gmail.com (Majid Muttashar).

1. Introduction

1.1 General

In recent years, fibre reinforced polymers (FRP) have been used in the construction industry due to its advantageous properties such as high stiffness, strength-to-weight ratios, resistance to corrosion and easy installation [1]. However, their relatively low elastic modulus as well as thin-walled sections lead to structural design being governed by deflection and buckling limitations rather than strength [2, 3]. These limitations of FRP composite sections can be overcome by infilling with concrete. In such hybrid systems, the deformation capacity is increased by the combined action between the concrete and the thin-walled FRP tube.

Concrete filled FRP tubes (CFFT) became a popular form of hybrid structural elements in rehabilitation or in new construction. In fact, extensive studies have been conducted to investigate the behaviour of CFFTs for bridge columns and piles applications [4-11]. Most of these studies have proven the ability of this system to take advantage of the confinement provided by the composite shell to the concrete core and the linear elastic nature of the composite section. Similar research has been conducted to investigate the confinement effect of FRP composite on the concrete core [12, 13]. These researches showed that FRP confinement has a significant effect on the behaviour of concrete under axial compression. Consequently, various models have been developed [14, 15] to predict the stress – strain behaviour of FRP – confined concrete.

The growing popularity of using concrete filled FRP for compression members has motivated researchers to expand the investigation of the system feasibility for bridge beam applications. Under flexural loading, Roeder et al. [16] found that the concrete infill increases local buckling resistance by stiffening the walls of the FRP tube. Davol et al. [17] performed bending tests of large –scale circular FRP shells filled with 45 MPa concrete. They found that increasing the amount of hoop plies around the specimen prevents the occurrence of local buckling on the compression side. Similarly, Fam and Rizkalla [18] carried out large scale flexural tests on hollow and concrete filled GFRP circular tubes wherein the effect of wall thickness ratios with a range of concrete infill strength between 30 and 60 MPa were examined. They reported that the flexural behaviour of concrete filled GFRP circular tubes is affected by the concrete compressive strength and is highly dependent on the stiffness and diameter – to – thickness ratio of the tube. Prior to this, Mirmiran and Shahawy [6] conducted experiments to investigate the flexural behaviour of concrete – filled FRP tubes as an alternative to the conventional reinforced concrete elements. In addition, Fam et al. [19]

studied the behaviour of CFFT box beam to replace the reinforced concrete beam. The results showed that the performance of the concrete filled beams is similar to or better than the conventional reinforced concrete elements. Chen and El-Hacha [20] introduced a new hybrid bridge girder system fabricated from FRP and ultra–high performance concrete (138 MPa). Their results showed that de-bonding at concrete-FRP interface is the main failure mode and it occurs prior to the expected load for flexural failure. Most recently, Aydin and Saribiyik [21] studied the effect of the adherence between concrete and GFRP profile on the flexural behaviour using sand particles and epoxy which are pasted in the interior surface of the profile. The results indicated that the flexural strength and fracture toughness significantly increased compared to the hollow GFRP section.

Previous studies focussed on using concrete of compressive strength in a range between 30 to 138 MPa to fill the FRP tubes in order to enhance the overall behaviour of the hybrid beams. To the authors' knowledge, there are no studies conducted investigating the potential use of low strength concrete as an infill to the GFRP tube beams. This study investigates the flexural behaviour of hollow and concrete filled square pultruded GFRP tubes. Four-point static bending test was conducted to evaluate the strength, stiffness and failure mechanisms of the concrete filled pultruded GFRP tubes. An analytical model based on force equilibrium, strain compatibility, linear elastic behaviour of FRP and partial stress – strain confinement model for concrete is adopted to predict the behaviour of the tested beams. The results from the theoretical modelling are then compared with the experiment results.

1.2 **Research motivation**

The importance and suitability of concrete filled FRP tubes for compression members has been demonstrated by many researchers. On the other hand, limited studies have been conducted exploring the use of this hybrid system for flexural members [18, 19, 22, 23]. These studies focussed on using concrete of high compressive strength to fill the FRP tubes. However, the cost of high strength concrete infill did not justify the enhancement in the stiffness and strength capacities of the hybrid beams. This study aims at investigating the influence of concrete infill strength on the flexural behaviour of pultruded GFRP square beams including low strength concrete to determine the optimal compressive strength that will result in enhanced strength and stiffness compared to hollow FRP tubes.

2. Experimental program

2.1 Properties of GFRP tubes and concrete

Square pultruded GFRP sections (125 mm x 125 mm x 6.5 mm thickness) produced by Wagner's Composite Fibre Technologies (WCFT), Australia were used in this study. The tubes were produced using pultrusion process with vinyl ester resin and E-glass fibre reinforcement. Burnout test conducted as per ISO 1172 [24] revealed that the density and the fibre volume fraction are 2050 kg/m^3 and 78% by weight, respectively. Table 1 shows the mechanical properties of the pultruded GFRP profiles. The elastic modulus and shear modulus of the square pultruded GFRP sections were determined previously by Muttashar et al. [25] and are listed in Table 1. On the other hand, coupon tests were conducted to determine the compressive and tensile strength properties for the sections.

Table 1. Properties of the pultruded GFRP profiles.

Concrete with three different strengths were used as infill in the pultruded sections. Five plain concrete cylinders have been sampled from each batch of three types of concrete and cured under the same conditions as the beam specimens. The 28 day average compressive strengths for the three types of concrete were 10, 37.5 and 43.5 MPa, respectively.

2.2 Test specimens

In the experimental works, three hollow GFRP sections and six filled sections were used to investigate the flexural behaviour. The total length of the beams was 2000 mm. Table 2 shows the details of specimens' identification and concrete strength. The specimens were identified using the code listed in the table. The term H-0 indicates the hollow geometry, whereas, H-10, H-37 and H-43 represent GFRP beams filled with concrete having 10, 37 and 43 MPa compressive strength respectively.

Table 2. Details of specimen identification and concrete strength of the tested beams.

2.3 Instrumentation and test setup

Four – point bending test was performed over a simply supported clear span of 1800 mm following the ASTM D7250 [26]. The load was applied at two points with a load span of 300 mm. Figure 1 shows the details of the experimental set up. The load was applied using a 400 kN capacity universal testing machine at a load rate of 3 mm/min. Steel plates were provided at the support and loading points to minimise indentation failure. Four uniaxial strain gauges (types PFL-20-11-1L-120) were used to measure the strain on the top and bottom faces of the beam. The mid-span deflection was measured using a laser displacement transducer. The applied load and the displacement were recorded using "System 5000" data acquisition

system. All specimens were tested up to failure to observe the failure mechanisms of the beam.

Figure 1. Details of experimental set up.

3. Test results and discussion

3.1 Load – deflection behaviour

The load - displacement behaviour of the tested beams is presented in Figure 2. As expected, the hollow beams (H-0) showed a linear elastic behaviour until failure at a load of 80.8 kN and a corresponding mid – span deflection of 39.5 mm. Consequently, the average ultimate flexural stress at the top and bottom of the tested beams was 291 MPa. This value is approximately 45% and 39% of the compression and tension failure stresses determined from coupon test of the GFRP profile, respectively. The ultimate strength of the GFRP profile was not achieved due to the compressive buckling of the top flange at the constant moment region which led to separation of the web-flange junction, followed by premature buckling, delamination and crushing in the web as shown in Figure 3. On the other hand, bilinear load – deflection curves were observed for GFRP beams with concrete infill. However, the first part of the curves is insignificant as it forms approximately 3% of the total value (segment A of the curve) as shown in Figure 2. The curve starts with a high stiffness as the entire concrete cross section is effective. However, once the flexural tensile cracking occurred, the stiffness was reduced but remained almost constant until failure. The H-10, H-37 and H-43 beams failed at an applied load of 163 kN, 189 kN and 195 kN, respectively, as shown in Figure 2.

There was a significant increase (100 to 141 % higher) in the flexural strength for the filled sections in comparison to those of the hollow sections for all concrete types. This increase reflects the contribution of the concrete core to the section's capacity by restricting and delaying the local buckling of the GFRP tube, thereby increasing the section ductility and strength. With the increase in concrete strength from 10 to 43.5MPa (335% increase), however, the improvement in sections' strength is only 19%. This is attributed to two important factors. Firstly, the brittleness of concrete increases with increasing strength, which changes the concrete crack patterns from heterogenic micro- cracks to localized macro - cracks. Secondly, the overall behaviour of the filled beams was controlled by the behaviour of the outside tube. With the internal support provided by concrete core, the pultruded profile is more stable and has smaller tendency to buckle which results in a higher load carrying capacity than hollow tubes. These results are in good agreement with the results reported by Vincent and Ozbakkaloglu [27] when they studied the influence of concrete strength on axial

compressive behaviour of FRP tubes filled with normal, high and ultra-high strength concrete. They concluded that the axial performance of FRP – confined concrete reduces as the concrete strength increases. From the current study, this result suggests that the effect of the compressive strength (for 10 to 43.5 MPa) of infill on the section capacity and stiffness is minimal for the tested beams. This finding is in contrast with the parametric study conducted by Fam and Rizkalla [18]. They reported that increasing the compressive strength of concrete from 20 to 80 MPa resulting in decreasing of the section capacity with noticeable increase in the stiffness. The reported difference in behaviour is more likely to be due to their assumption of using unconfined stress – strain concrete model to predict the behaviour. Figurer 4 shows the strain distribution through the depth of the section at mid - span which clearly shows that the neutral axis depth is higher for lower concrete strength and lower for higher compressive strength. It is obvious that modulus of elasticity becomes higher for high strength concrete however the moment of inertia becomes lower due to the changes of the neutral axis depth. For example, the neutral axis depth is at a distance of 58 mm from the top of the section for H-10, 53.5 mm for H-37 and 51.5 mm for H-43, at 60 kN.m moment capacity. It is noted that 60 kN.m moment capacity corresponds to a 160 kN applied load. This result also suggests that the area of concrete contributing to compressive force is lower for a higher strength than a lower strength concrete to achieve internal force equilibrium. Consequently, the ultimate load of the beam is slightly affected by the concrete compressive strength. Even reaching the maximum compressive stress in concrete, the concrete core remains intact and stabilises the hollow GFRP profile until the failure causing some crushing for H-43. This behaviour demonstrates that some level of confinement in concrete is present.

Figure 2. Failure mode of hollow beams

Figure 3. Load - displacement behaviour of the tested beams

Figure 4. Mid - span strain distribution at moment capacity of 60 (kN. m) for all beams.

Figure 5 shows the flexural stiffness of hollow and concrete filled (uncracked and cracked) beams. The average flexural stiffness, *EI* of the hollow section is 2.38 x 10^{11}N.mm^2. This value was calculated using the equation:

$$EI = \frac{Pa}{48\,\Delta}\,(3L^2 - 4a^2) \qquad (1)$$

where *EI* is the effective flexural stiffness in N.mm^2; *P* is the applied load in N; *a* is the shear span which is the distance between the support and the nearest point load in mm; Δ is the mid- span deflection in mm; and *L* is the span in mm. As mentioned earlier in this section, due to the trivial ratio of the first part of the curves in Figure 3, equation 1 can be used to calculate

the flexural stiffness of the infilled sections. The uncracked flexural stiffness of the filled beams is 3.19 x 10^{11} N.mm^2 for 10 MPa concrete and 4.19 x 10^{11} N.mm^2 for 43 MPa concrete. This result showed that the flexural stiffness of beams with uncracked concrete infill is higher by 34, 55 and 75% for 10, 37 and 43 MPa, respectively, compared to the hollow section. On the other hand, the flexural tensile cracking of the concrete core results in a section with a reduced moment of inertia. In this condition, the flexural stiffness of the beam for all concrete strengths is approximately 26% higher than the hollow section. Interestingly, the flexural stiffness of the beams with concrete infill is almost same. This can be explained by the extent of the depth of the cracked concrete as explained previously. It can also be seen in Figure 4 that at specific load level, H-10 showed higher compression strain reading compared with H-37 and H-43 while the tension strain seems to be similar for all concrete types. Compared with H-37 and H-43, higher strain reading for H-10 resulting from higher deflection experienced by this beam can be observed. With an increase in the applied load there is an increase in the deflection of the filled beams. The results show that at the specific load level, the mid – span deflection were 60.6, 62.3 and 63.9 mm for H-10, H-37 and H-43, respectively. The main reason for this behaviour is the difference in modulus of elasticity of the concrete core. This is evident from the experimental results that filling the tube with low strength concrete resulted in higher curvature compared with other concrete strengths as shown in Figure 6. On the other hand, it should be noted that due to the effect of the cracked section, the bottom fibre showed approximately similar tensile strain reading which result in different compression strain values to maintain the balance of the internal forces depending on the strength of the concrete core. This behaviour explains the slightly lower failure load of H-10 compared to H-37 and H-43. Consequently, the beam failed when the top fibre of the GFRP tube reaches a compressive strain near or equal to the maximum compressive strain determined from the coupon test.

Figure 5. Comparison of flexural stiffness.

Figure 6. Moment - curvature behaviour of the tested beams.

3.2 Strain response

Figure 7 shows the load and strain (at mid span at the topmost and bottom most section) relationship of the hollow and concrete filled beams. It can be seen that the hollow section failed at a compressive strain of 3140 microstrains and tensile strain of 6100 microstrains. With increasing load, however, the measured strain tend to become positive indicating that the top surface is shifting from compression to tension as shown in figure 7a. This behaviour

indicates the initiation of the local buckling of the tube. For beams with concrete infill, a slight decrease in stiffness at a tensile strain of 140 microstrains (load between 3.1 and 4 .4 kN) was observed. This decrease in stiffness can be related to the initiation of tensile cracks in the concrete core. The filled sections failed at tensile strains of 12400, 14800 and 14820 microstrains for H-10, H-37 and H-43, respectively as shown in figure 7b. These strain levels were approximately 77, 92 and 93% of the maximum strain of pultruded section determined from the test of coupons (Table 1). Thus, it is concluded that no tension failure had occurred at the onset of the final failure. On the other hand, the maximum measured compression strains were 11100, 11200 and 11250 microstrains for H-10, H-37 and H-43, respectively. These values are 97, 98 and 98.5% of the ultimate compressive strains of the pultruded GFRP tubes which indicates that the filled sections failed at onset of the compression failure. Furthermore, the slight differences between the failure compression strains of the filled sections indicate that for all concrete strengths, the concrete core prevents the occurrence of premature local buckling and supported the top wall of the section. As a result, the section failed at strain of 11200 microstrains which represents the highest compression strain achieved in coupon tests. It can also be noticed from Figure 7 that there was no clear drop in the curve until failure with good strain distribution on both sides indicating that there was no major slip occurred between concrete and the GFRP tube.

Figure 7. Load - strain behaviour of the tested beams: (a) hollow, (b) filled

3.3 Failure mode

Figure 8 (a-d) shows the typical mode of failure of the hollow and filled beams tested under 4-point bending. The experimental results illustrate that the hollow beams failed in a brittle manner. The failure started at the web – flange junctions and followed by premature buckling and crushing in the webs as shown in figure 8a. Similar behaviour has been reported in the literature [25, 28, 29] on flexural behaviour of 125, 100, 76 mm square pultruded GFRP beams. The main reason for this failure is the local buckling in the thin wall which results in material delamination and cracking of the fibres along the edges of the beam under the load application.

Figure 8(b), (c) and (d) show the failure modes of GFRP beams filled with 10, 37.5 and 43.5 concrete strength, respectively. The failure of all filled beams was due to flexural compression at the constant moment region including cracks in the fibres in the transverse direction. It was observed that delamination crack happened at the compression surface which later progressed into the sides. The complete failure occurred after the fibre cracking in

the compression side (at strain level approximately 11200 microstrains). This strain level is far greater than the failure strain of the hollow section (3140 microstrains) which indicates that the concrete infill prevented the occurrence of local buckling.

The crack pattern in the concrete core was examined by carefully removing the GFRP tube after failure as shown in figure 9. The figure clearly shows that flexural cracks were developed at the bottom of the beam between the loading points. Also, the cracks propagated up to the depth of the concrete infill. H-37 and H-43 beams showed distinct flexural cracks as shown in Figure. 9b and c whereas H-10 beam shows fine cracks as can be seen from Figure 9a. A similar behaviour was reported by Vincent and Ozbakkaloglu [27] and it can be attributed to the brittleness of concrete which increases with increasing concrete compressive strength. As a result, the concrete crack pattern changes from fine microcracks to localized macrocracks. It is also interesting to note that although the complete failure occurred at a strain level of 11200 microstrains (which is too far away from concrete compression strain of 3000 microstrains), there was no concrete crushing observed at the compression side except the case of section H-43 which might have happened after the final failure. This suggests that there is a partial confinement by the GFRP section which in turn kept the concrete under compression intact until failure of the tube.

Figure 8. Failure modes of the tested beams.

Figure 9. Crack pattern at failure of the tested beams.

4. Theoretical analysis

4.1 Analytical model

Fibre model analysis (FMA) implemented previously [30] for the analysis of sandwich composite beams is used to predict the flexural behaviour of the concrete filled GFRP beams. The analytical model (as shown in figure 10) involves the determination of the position of the neutral axis for a given strain of the extreme compression fibre by using the principles of strain compatibility and cross sectional forces equilibrium. The analytical procedure starts by dividing the cross- section into a number of layers. Based on the appropriate stress – strain model for each material, the stress for each layer is determined depending on the corresponding strain. The internal force at each layer is then calculated by multiplying the stress by the area of layer and the bending moment is obtained by multiplying the force by the distance of the layer from the neutral axis of the section. Using this procedure, the flexural behaviour is determined, and then compared with experimental results.

The assumptions in the analysis include:

1) Euler – Bernoulli beam theory
2) Strain distribution throughout the depth of the section is linear
3) Perfect bond between pultruded section and the concrete core
4) Confinement effect is considered
5) Cracked analysis is implemented
6) Pultruded GFRP section behaves linear elastically until failure
7) Stress-strain curve for the GFRP tube was based on full section behaviour (Figure 11).

The confinement effect plays an important role in choosing the appropriate stress – strain behaviour for concrete. This is considered in the analysis of the flexural behaviour of the concrete filled GFRP tubes. The existing design-oriented stress-strain models for FRP-confined concrete typically followed a bilinear stress-strain curve [31-33]. The bilinear curve consists of a parabolic ascending branch followed by straight line to describe both the ascending and descending branches of the stress-strain curves of confined concrete [34, 35]. The parabolic portion is commonly used in several codes of practice such as BS 8110 and Eurocode 2 [35] which was originally proposed by Kent and Park [36]. This curve used to describe the ascending portion of the stress-strain curve of unconfined concrete given by the following equation.

$$\sigma_c = f'_{co}\left[\frac{2\varepsilon_c}{\varepsilon_{co}} - \left(\frac{\varepsilon_c}{\varepsilon_{co}}\right)^2\right] \qquad when\ \varepsilon_c \le \varepsilon_{co} \tag{2}$$

where σ_c in MPa and ε_c represent the stress and strain, respectively, while f'_{co} in MPa and ε_{co} are the unconfined concrete cylinder strength and the corresponding strain, respectively. For the definition of the linear second part of the curve, several researches were conducted to determine its slope. In fact, all the conducted research agreed that the FRP confinement is activated once micro-cracks in concrete are initiated under loading which means it is important to determine the correct slope of the second part. Existing studies shows that due to the presence of a strain gradient over the section in flexural, the confinement of FRP to concrete is less effective in sections under bending than in sections under compression [18, 37]. However, it is still significant and important to be considered in predicting the load – carrying capacity of the CFFTs [38, 39]. Fam et al. [40] suggested that for sections under pure bending unconfined stress-strain curve can be used by considering the effect of strain gradient on the effectiveness of concrete confinement. As a result, they recommended using an ultimate strain higher than that of unconfined concrete,

however, their direct use of unconfined stress-strain concrete model result in underestimation of the load- carrying capacity of the filled beams.

In the present study, a similar elastic modulus in both tension and compression has been assumed for the concrete. Tensile cracking was assumed to occur at a tensile strain of 120 microstrains for H-10, H-37 and H-43, respectively. The contribution of the concrete in tension is neglected after tensile cracking. Partial confinement model is used in this study which is composed of a parabolic ascending branch following [34] and a horizontal (zero slope) branch following [40] which provides the lower bound for the variable confinement model as described in the following equation:

$$\sigma_c = f'_{co} \qquad when\ \varepsilon_c > \varepsilon_{co} \tag{3}$$

The partial confinement model is thus described by equations (2) and (3) as shown in Figure 12. Same model was proposed [38] for hybrid FRP – concrete – steel double skin tubular sections under bending which showed close predictions withthe test results. Based on the experimental observations, the ductility and strain of concrete are increased significantly beyond 0.003. It is also well established that failure of concrete filled FRP tubes system is normally governed by local buckling failure of the FRP tube in the compression region before complete failure of the concrete inside. For this failure mode, ε_{co} can be conservatively assumed to be equal to the design ultimate axial strain obtained from the axial compression tests of hollow FRP tubes due to the fact that the failure strain of the FRP tubes in the filled beams is more than that of hollow tubes.

Figure 10. Assumed strain and stress distribution in the FMA.

Figure 11. Stress – strain model for GFRP tube.

Figure 12. Stress – strain model for confined concrete.

4.2 Failure load prediction

The cracking and failure load of the hollow and filled sections were predicted using FMA described in the previous section. In the experimental program, it was observed that the compression failure of the hollow and filled pultruded sections is the dominant mode of failure. For hollow sections, the top fibre compression strain reached 6100 microstrains while the corresponding strain was 11200 microstrains for the filled sections regardless of the concrete compressive strength. The main reason for the failure of the hollow GFRP profile at lower strain is the local buckling effect. Introducing the concrete infill to the section prevented the local buckling of the GFRP tube. As a result, the compression strain reached its highest value. The cracking load was predicted as the load corresponding to a strain of 120

microstrains which was calculated based on the cracking strength of concrete and the modulus of elasticity of the concrete. According to the Australian standard AS 3600 [41], the cracking strength of concrete f_{cr} in MPa can be calculated as follows:

$$f_{cr} = 0.6\sqrt{f_c'} \quad (4)$$

where f_c' is the concrete compressive strength at 28 days in MPa. Table 3 shows the predicted cracking and failure loads along with corresponding values. Partial confinement model using equations 2 and 3 has been used to simulate the stress – strain behaviour of the concrete core. The results indicate that the failure loads of the concrete filled beams can be predicted well using the elastic properties of the full-section GFRP profile and the strength properties determined from coupon tests together with the use of the partial confinement stress –strain model. The predicted cracking and failure loads of all specimens are less than 1% different from the measured values.

Table 3. Experimental and predicted failure load of hollow and filled pultruded section

4.3 Load – deflection relationship

The FMA was extended to predict the load – deflection behaviour of the hollow and filled pultruded sections using shear deformation theory proposed by Timoshenko in 1921 [42] . In this theory, the contribution of bending and shear deflection has been account for in calculating total deflection. The total deflection at mid span in a simply supported beam under four – point bending can be calculated by:

$$\Delta = M\left[\frac{a^2}{3EI} + \frac{1}{2EI}\left(\frac{L^2}{4} - a^2\right)\right] + \frac{Pa}{2KGA} \quad (5)$$

where Δ is the deflection at mid span in mm, M is the applied moment in N.mm, EI is the flexural stiffness in N.mm^2, GA is the shear stiffness (or transverse shear rigidity) in N and K is the shear coefficient. Two configurations of the test specimen – hollow and filled - have been used. As a consequence, two different K values need to be implemented in the calculations. For homogenous and hollow box profile, K was calculated using the equation recommended by Bank [43]:

$$K = \frac{80}{192 + \left(-12 * \upsilon * G/E\right)} \quad (6)$$

Where E is the modulus of elasticity in MPa, G is the shear modulus in MPa and υ is the Poisson's ratio. It is well known that the transverse shear rigidity is a function of the shear flow across the section, which depends on the thickness of the cross section. As a result, due to the change of the section configuration from hollow to filled, all cross section is assumed

to contribute in the shear deflection calculation. Thus, a value of $K = 1$ is used for the case of filled section. In equation 6, υ, G and E refer to the longitudinal Poisson's ratio, shear modulus in MPa and Modulus of Elasticity of the section in MPa, respectively. Figure 13(a – d) shows comparisons between the predicted and the experimental mid span load – deflection curves for the hollow and filled beams. Using GFRP properties determined from the full scale test and concrete properties, the theoretical results agree well with the experimental test results up to failure. The figure shows that the difference between the theoretical and the experimental results are less than 1% for all beams. Similarly, it is evident from the curves that the assumed value of $K = 1$ for beams with concrete infill was valid for all concrete strength.

Figure 13. Comparisons of mid span load – deflection curves

4.4 Load – strain relationship

Figure 14(a-d) shows comparisons of predicted and experimental load – strain curves for hollow and filled sections. The strain values presented are those of the extreme fibre at the mid-span. The experimental results shows a linear relationship in tension and bilinear in compression side. For the hollow section, there is a slight difference between the analytical and the experimental results in the compression side. The main reason for this divergence is the effect of local buckling which is not considered in the theoretical model. On the other hand, the analytical results agree well with predicted load – strain relation in tension.

The good agreement between the analytical and experimental results for all concrete types confirms the validity of the partial confined model in predicting the load – strain relation. Similarly, the load – strain relationship shows a higher strain in the tension compared with compression side, which confirms the tensile cracking of the concrete and decreasing its contribution in the flexural stiffness. Finally, the assumption of compatibility of strains through the depth of the section and the equilibrium of the internal force resultants are valid.

Figure 14. Comparisons of load – strain curves

5. Conclusions

This study has presented the results of four point bending tests on hybrid concrete filled GFRP tubes. The main parameter examined in this study is the compressive strength of concrete core. A simple theoretical model was implemented and used to predict the behaviour of the tested beams. Based on the results, the following conclusions can be drawn:

- Hollow beams failed due to premature buckling and web crushing of the GFRP tube at 291 MPa. This level of stress is only 45% of the compressive strength determined from the coupon tests.
- The concrete filled GFRP sections failed at a load 100 to 141 % higher than its hollow counterpart and exhibited 25% higher stiffness. The failure of these beams was compressive failure of the GFRP tube at a strain similar to the compressive strain determined from the coupon tests.
- The increase in concrete compressive strength from a low 10 MPa to a high strength 43.5 MPa increased the ultimate load by 19%. Similarly, the flexural stiffness of the beam with concrete infill is almost the same after the initiation of the flexural tension cracks in the concrete core.
- Use of low strength concrete can be considered as a practical solution to fill the GFRP tubes to prevent local buckling and improve the overall flexural behaviour.
- The simplified Fibre Model Analysis can accurately predict the flexural behaviour of the hollow and concrete filled GFRP tubes. For the hybrid beams, partial confinement of the concrete infill should be considered.
- The theoretical prediction of the concrete cracking and the failure loads for the concrete filled GFRP tubes using the elastic properties of the full-section GFRP tubes and the strength properties determined from the coupon test is in close agreement with the experimental results.

Acknowledgement

The authors are grateful to Wagner's Composite Fibre Technologies (WCFT), Australia for providing all the GFRP tubes in the experimental programme. The first author would like to acknowledge the financial support by the Ministry of Higher Education and Scientific Research-Iraq.

References

[1] Hollaway L. A review of the present and future utilisation of FRP composites in the civil infrastructure with reference to their important in-service properties. Construction and Building Materials. 2010;24:2419-45.

[2] Ascione L, Berardi VP, Giordano A, Spadea S. Buckling failure modes of FRP thin-walled beams. Composites Part B: Engineering. 2013;47:357-64.

[3] Neto A, Rovere H. Flexural stiffness characterization of fiber reinforced plastic (FRP) pultruded beams. Composite Structures. 2007;81:274-82.

[4] Fam AZ, Rizkalla SH. Confinement model for axially loaded concrete confined by circular fiber-reinforced polymer tubes. ACI Structural Journal. 2001;98.
[5] Fam AZ, Rizkalla SH. Behavior of axially loaded concrete-filled circular fiber-reinforced polymer tubes. ACI Structural Journal. 2001;98.
[6] Mirmiran A, Shahawy M. A new concrete-filled hollow FRP composite column. Composites Part B: Engineering. 1996;27:263-8.
[7] Mohamed HM, Masmoudi R. Axial load capacity of concrete-filled FRP tube columns: Experimental versus theoretical predictions. Journal of Composites for Construction. 2010;14:231-43.
[8] Ozbakkaloglu T. Axial compressive behavior of square and rectangular high-strength concrete-filled FRP tubes. Journal of Composites for Construction. 2012;17:151-61.
[9] Ozbakkaloglu T, Oehlers DJ. Concrete-filled square and rectangular FRP tubes under axial compression. Journal of Composites for Construction. 2008;12:469-77.
[10] Ozbakkaloglu T. Concrete-filled FRP tubes: Manufacture and testing of new forms designed for improved performance. Journal of Composites for Construction. 2012;17:280-91.
[11] Ozbakkaloglu T, Akin E. Behavior of FRP-confined normal-and high-strength concrete under cyclic axial compression. Journal of Composites for Construction. 2011;16:451-63.
[12] Xiao Y, Wu H. Compressive behavior of concrete confined by carbon fiber composite jackets. Journal of Materials in Civil Engineering. 2000;12:139-46.
[13] Teng J, Lam L. Behavior and modeling of fiber reinforced polymer-confined concrete. Journal of structural engineering. 2004;130:1713-23.
[14] Yu T, Teng J. Design of concrete-filled FRP tubular columns: provisions in the Chinese technical code for infrastructure application of FRP composites. Journal of Composites for Construction. 2010.
[15] Binici B. An analytical model for stress–strain behavior of confined concrete. Engineering structures. 2005;27:1040-51.
[16] Roeder CW, Lehman DE, Bishop E. Strength and stiffness of circular concrete-filled tubes. Journal of structural engineering. 2010;136:1545-53.
[17] Davol A, Burgueno R, Seible F. Flexural behavior of circular concrete filled FRP shells. Journal of structural engineering. 2001;127:810-7.
[18] Fam AZ, Rizkalla SH. Flexural behavior of concrete-filled fiber-reinforced polymer circular tubes. Journal of Composites for Construction. 2002;6:123-32.
[19] Fam A, Cole B, Mandal S. Composite tubes as an alternative to steel spirals for concrete members in bending and shear. Construction and Building Materials. 2007;21:347-55.
[20] Chen DS, El-Hacha R. Flexural behaviour of hybrid FRP-UHPC girders under static loading. Proceedings of 8th International Conference on Short and Medium Span Bridge Niagara Falls, Canada2010.
[21] Aydin F, Saribiyik M. Investigation of flexural behaviors of hybrid beams formed with GFRP box section and concrete. Construction and Building Materials. 2013;41:563-9.
[22] Fam A, Flisak B, Rizkalla S. Experimental and analytical modeling of concrete-filled fiber-reinforced polymer tubes subjected to combined bending and axial loads. ACI Structural Journal. 2003;100.
[23] Mohamed HM, Masmoudi R. Flexural strength and behavior of steel and FRP-reinforced concrete-filled FRP tube beams. Engineering structures. 2010;32:3789-800.
[24] ISO 1172. Textile-glass-reinforced plastics, prepegs, moulding compounds and laminates: Determination of the textile-glass and mineral-filler content- Calcination methods. 1996.
[25] Muttashar M, Karunasena W, Manalo A, Lokuge W. Behaviour of hollow pultruded GFRP square beams with different shear span-to-depth ratios. Journal of Composite Materials. 2015:0021998315614993.
[26] ASTM D7250. ASTM D7250/D7250M-06 Standard practice for determine sandwich beam flexural and shear stiffeness. West Conshohocken, (PA): ASTM International; 2006.

[27] Vincent T, Ozbakkaloglu T. Influence of concrete strength and confinement method on axial compressive behavior of FRP confined high-and ultra high-strength concrete. Composites Part B: Engineering. 2013;50:413-28.
[28] Guades E, Aravinthan T, Islam MM. Characterisation of the mechanical properties of pultruded fibre-reinforced polymer tube. Materials & Design. 2014;63:305-15.
[29] Kumar P, Chandrashekhara K, Nanni A. Structural performance of a FRP bridge deck. Construction and Building Materials. 2004;18:35-47.
[30] Manalo A, Aravinthan T, Karunasena W, Islam M. Flexural behaviour of structural fibre composite sandwich beams in flatwise and edgewise positions. Composite Structures. 2010;92:984-95.
[31] Fardis MN, Khalili HH. FRP-encased concrete as a structural material. Magazine of Concrete Research. 1982;34:191-202.
[32] Samaan M, Mirmiran A, Shahawy M. Model of concrete confined by fiber composites. Journal of structural engineering. 1998.
[33] Saafi M, Toutanji H, Li Z. Behavior of concrete columns confined with fiber reinforced polymer tubes. ACI Materials Journal. 1999;96.
[34] Hognestad E. Study of combined bending and axial load in reinforced concrete members. University of Illinois Engineering Experiment Station Bulletin; no 399. 1951.
[35] Lam L, Teng J. Design-oriented stress–strain model for FRP-confined concrete. Construction and Building Materials. 2003;17:471-89.
[36] Kent DC, Park R. Flexural members with confined concrete. Journal of the Structural Division. 1971;97:1969-90.
[37] Wu Z, Li W, Sakuma N. Innovative externally bonded FRP/concrete hybrid flexural members. Composite Structures. 2006;72:289-300.
[38] Yu T, Wong Y, Teng J, Dong S, Lam E. Flexural behavior of hybrid FRP-concrete-steel double-skin tubular members. Journal of Composites for Construction. 2006;10:443-52.
[39] Mirmiran A, Shahawy M, Samaan M. Strength and ductility of hybrid FRP-concrete beam-columns. Journal of structural engineering. 1999;125:1085-93.
[40] Fam A, Flisak B, Rizkalla S. Experimental and analytical modeling of concrete-filled FRP tubes subjected to combined bending and axial loads. ACI Struct J. 2003;100:499-509.
[41] AS3600. concrete structure. Australian Standards 2009.
[42] Timoshenko SP, Young DH, Weaver W. Vibration problems in engineering. Vibration problems in engineering. 4th ed. ed. New York: Wiley; 1974.
[43] Bank LC. Composite for Construction Structural Design with FRP Materials. New Jersey: Jone Wiley & Sons, 2006.

All Figures

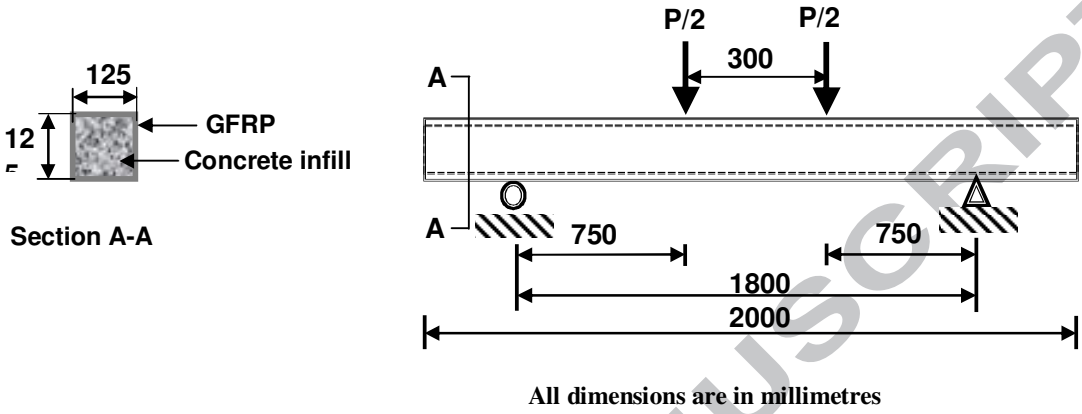

Figure 1. Details of experimental set up.

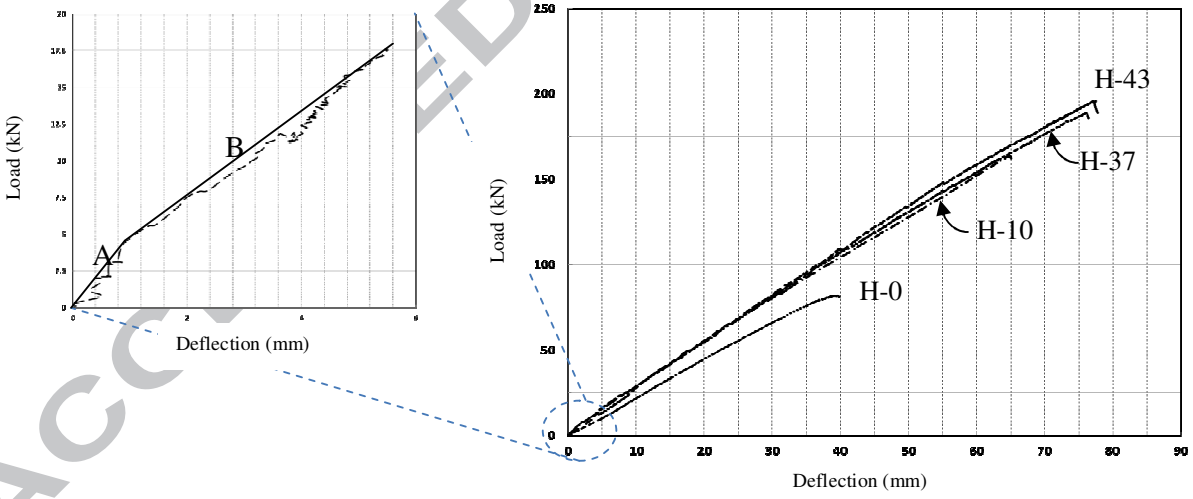

Figure 2. Load - displacement behaviour of the tested beams.

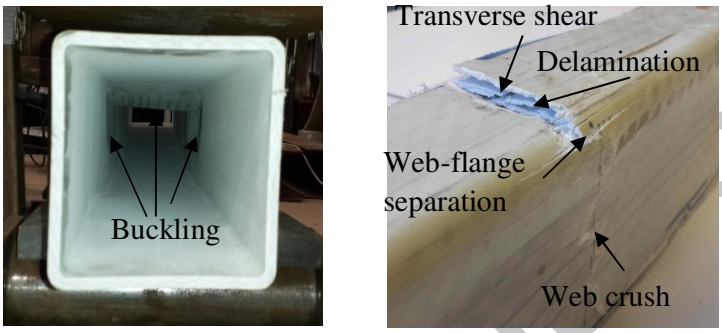

(a) Inside view (b) Outside view

Figure 3. Failure mode of the hollow beams.

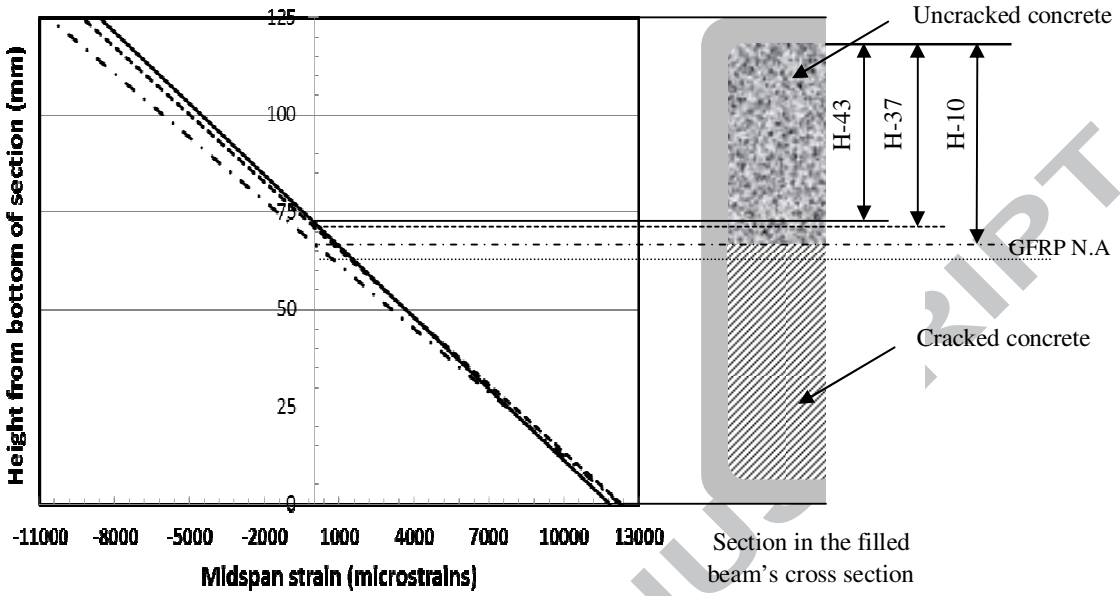

Figure 4. Mid - span strain distribution at moment capacity of 60 (kN. m) for all beams.

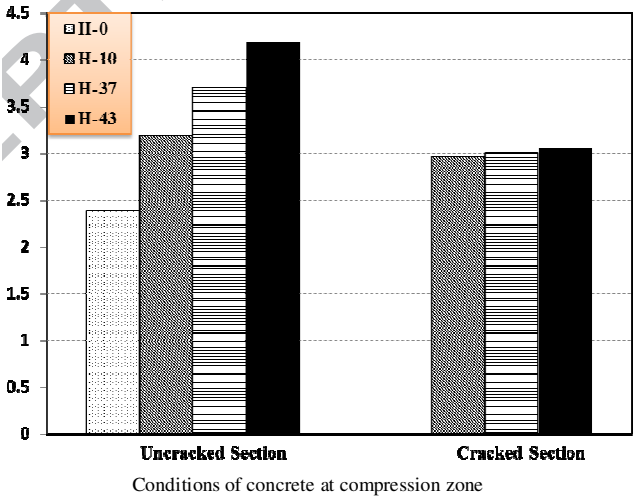

Figure 5. Comparison of flexural stiffness

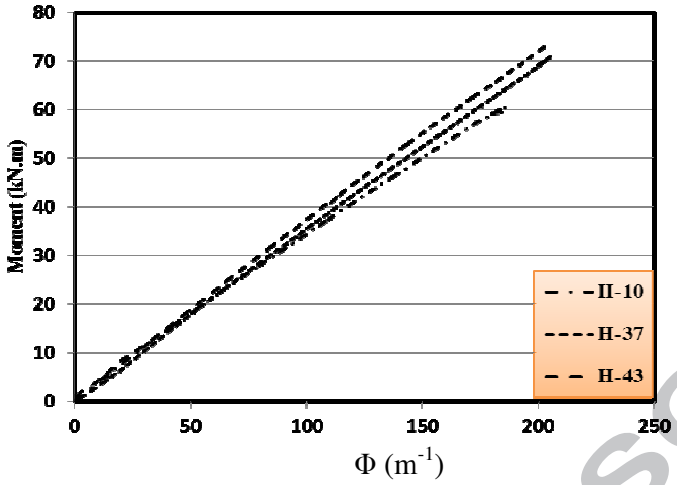

Figure 6. Moment - curvature behaviour of the tested beams.

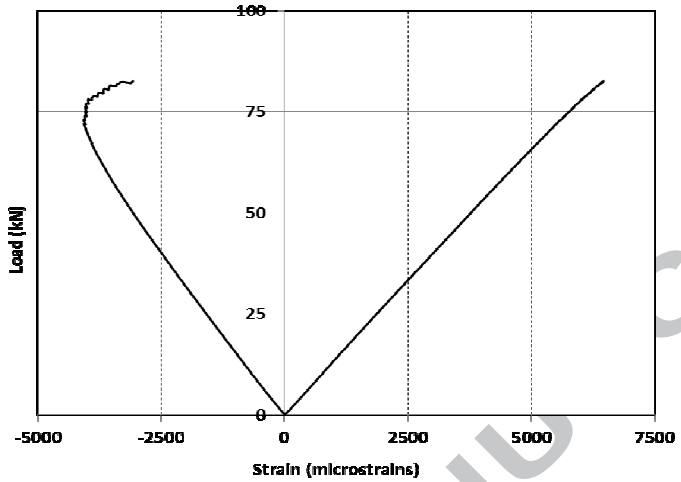

(a)

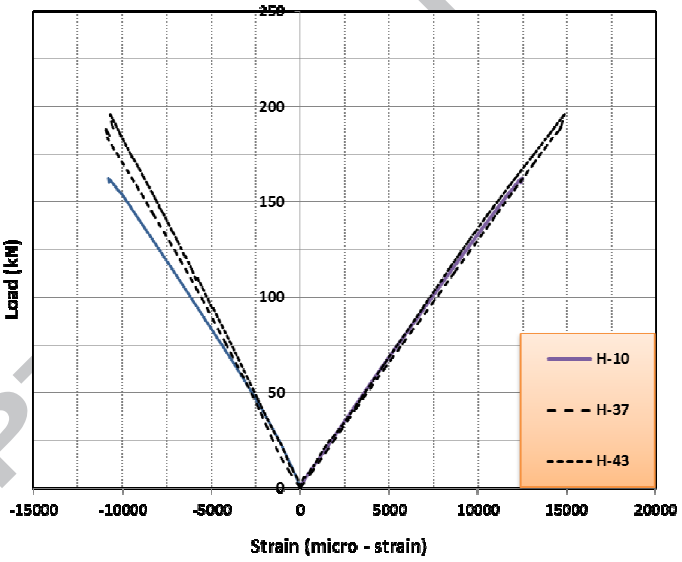

(b)

Figure 7. load - strain behaviour of the tested beams: (a) hollow, (b) filled.

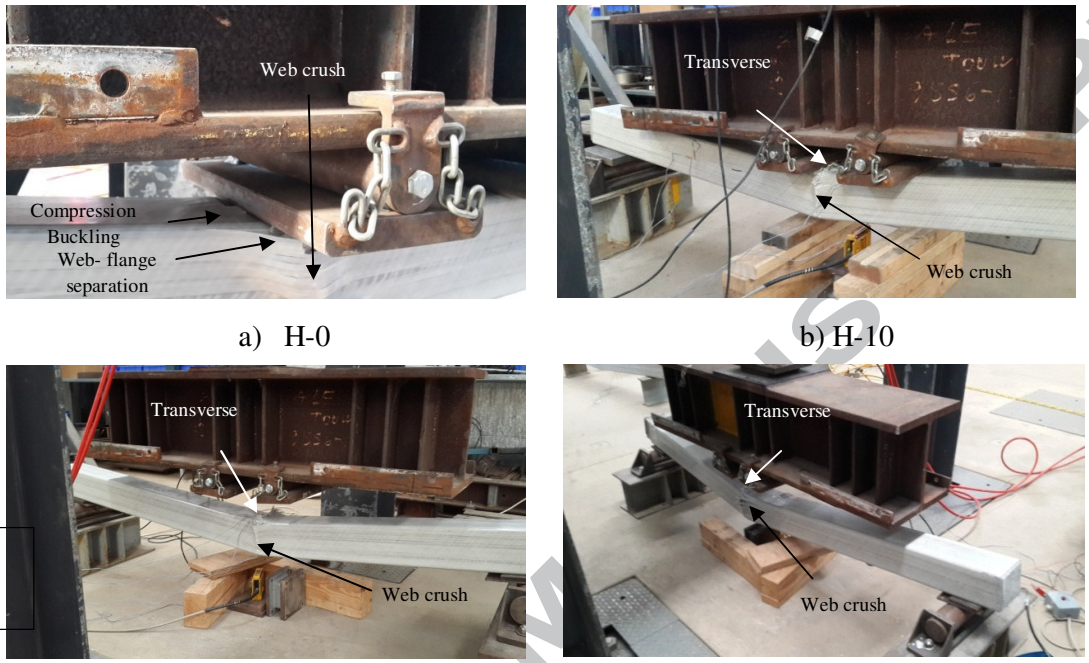

a) H-0 b) H-10

c) H-37 d) H-43

Figure 8. Failure modes of the tested beams.

a) H-10 b) H-37 c) H-43

Figure 9. Crack pattern at failure of the tested beams.

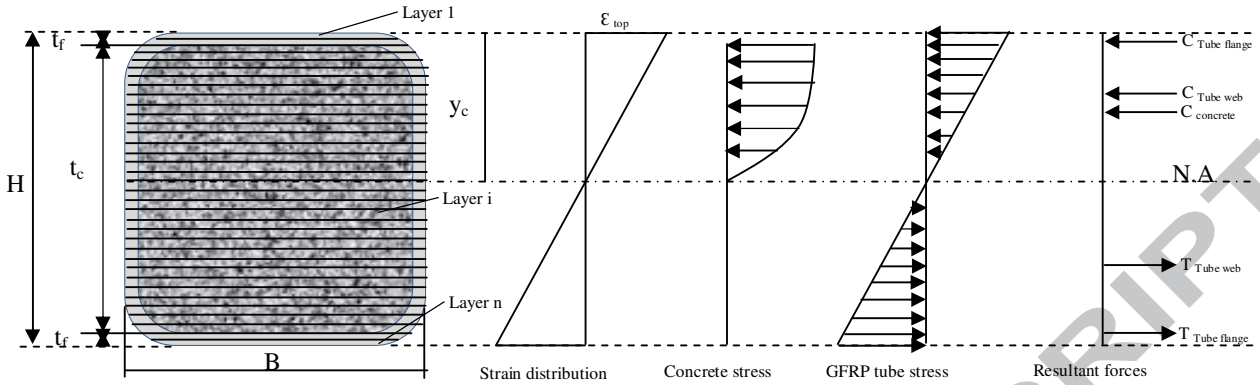

Figure 10. Assumed strain and stress distribution in the FMA.

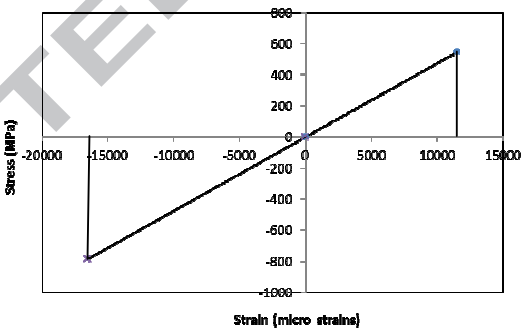

Figure 11. Stress – strain model for GFRP tube.

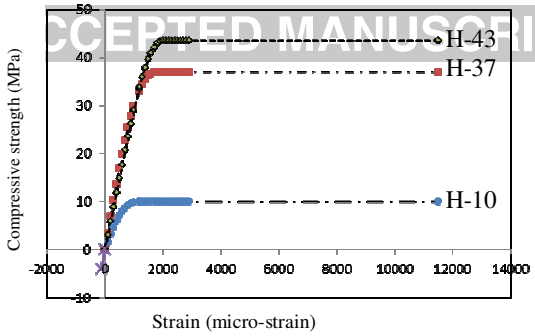

Figure 12. Stress – strain model for confined concrete.

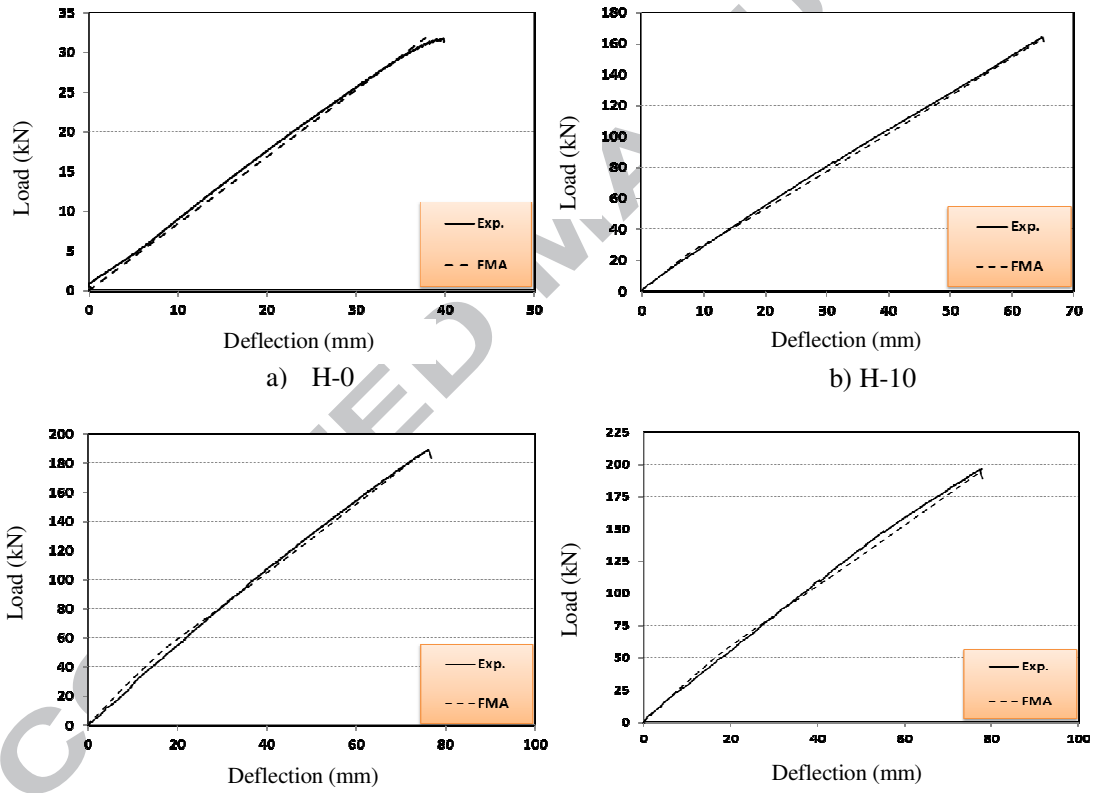

Figure 13. Comparisons of mid span load – deflection curves.

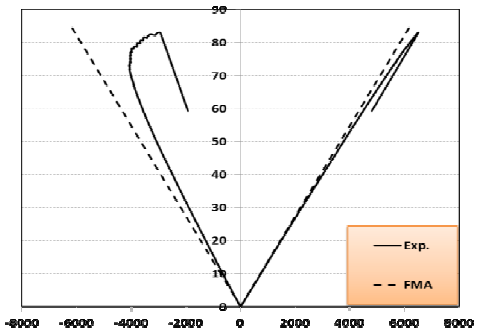

a) H-0

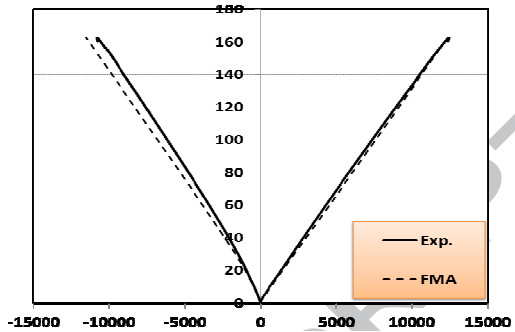

b) H-10

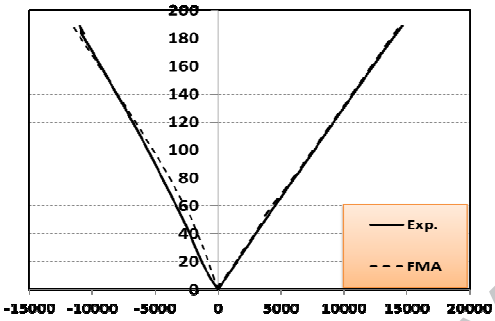

c) H-37

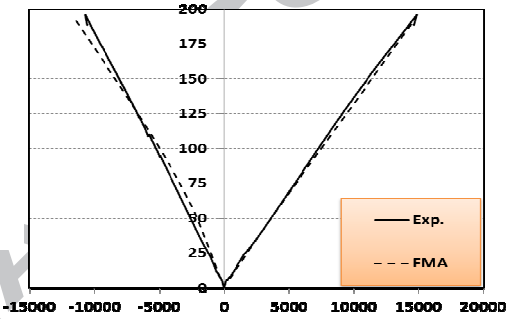

d) H-43

Figure 14. Comparisons of load – strain curves.

All Tables

Table 1. Properties of the pultruded GFRP profiles.

Material property	Symbol	Property value	unit
Density	ρ	2050	kg/m^3
Tensile stress	σ_t	596	MPa
Tensile strain	ε_t	16030	microstrain
Compressive stress	σ_c	550	MPa
Compressive strain	ε_c	11450	microstrain
Elastic modulus	*E*	47.2	GPa
Shear modulus	*G*	4	GPa

Table 2. Details of the test specimens.

Specimen ID	Description
	Concrete strength (MPa)
H-0	-
H-10	10
H-37	37.5
H-43	43.5

Table 3. Experimental and predicted failure load of hollow and filled pultruded section

Sample designation	Experimental load kN		Theoretical prediction kN	
	cracking	failure	cracking	failure
H-0	-	80.8	-	80.7
H-10	3.1	163	2.98	162.6
H-37	4.25	189	4.2	188.5
H-43	4.38	195	4.28	193.4